Modeling of subthreshold characteristics for undoped and doped deep nanoscale short channel double-gate MOSFETs*

Jin Xiaoshi(靳晓诗)[1,†], Liu Xi(刘溪)[1], Wu Meile(吴美乐)[1], Chuai Rongyan(揣荣岩)[1], Jung-Hee Lee[2], and Jong-Ho Lee[3]

[1]School of Information Science and Engineering, Shenyang University of Technology, Shenyang 110870, China
[2]School of EECS, Kyungpook National University, 1370 Sangyuk-Dong Buk-Gu, Daegu 702-701, Korea
[3]School of EECS Eng. and ISRC (Inter-University Semiconductor Research Center), Seoul National University, Shinlim-Dong, Kwanak-Gu, Seoul 151-742, Korea

Abstract: A model of subthreshold characteristics for both undoped and doped double-gate (DG) MOSFETs has been proposed. The models were developed based on solution of 2-D Poisson's equation using variable separation technique. Without any fitting parameters, our proposed models can exactly reflect the degraded subthreshold characteristics due to nanoscale channel length. Also, design parameters such as body thickness, gate oxide thickness and body doping concentrations can be directly reflected from our models. The models have been verified by comparing with device simulations' results and found very good agreement.

Key words: double-gate; MOSFETs; deep nanoscale; modeling
DOI: 10.1088/1674-4926/33/12/124003 **EEACC:** 2570

1. Introduction

Double-gate (DG) MOSFETs, a promising device structure which belongs to the multigate family has been considered as a candidate for next generation integrated circuit cells. Low power consumption can be realized due to near-ideal subthreshold characteristics (typically 60 mV/decade). It can be fabricated based on SOI technology which shows better performance compared to bulk CMOS technology due to the perfect isolation between individual devices. Latchup can be eliminated in SOI circuit. Also, it can be operated at lower voltages than conventional bulk CMOS devices. Therefore, DG MOSFETs have become a hot topic[1,2]. However, as the device channel length was reduced to sub-50 nm, even multigate devices show device characteristics' degradation due to short channel effect. In order to quantitively describe characteristics' degradation of nanoscale short channel DG MOSFETs, an accurate model should be developed. Analytical models of DG for 1-D model long channel DG have been derived[3−8]. However a 1-D model theoretically can not correctly reflect the 2-D potential distribution in the body region. Therefore, the short channel effect can not be reflected from the 1-D model either. In order to describe the influence of the short channel effect, a 2-D model should be given. 2-D models of threshold voltage and subthreshold swing for the undoped case have been given[9−12]. However, because the doped channel is an important design parameter which can adjust the threshold voltage, it should also be reflected directly from the model. A short channel doped model has been given, however, it's based on the solution of a 1-D Poisson's equation, and needs fitting parameters to adjust the model[13]. In this work, we proposed a subthreshold characteristics model which is based on the solution of a 2-D Poisson's equation. It can reflect the subthreshold characteristics' degradation due to channel length reduced to deep nanoscale. Our model also can give an exact subthreshold body potential distribution. Nanoscale design parameters such as channel length, body thickness, gate oxide thickness can be directly reflected from our proposed model. As a unified model, our models satisfy both undoped and doped cases. The models have been verified by comparing with device simulations' results using SILVACO[14] and found very good agreement.

2. Model derivations

Figure 1 shows a 2-D schematic view of DG MOSFET and the coordinate system. Take N-MOS as an example, the body is set to be doped with p-type impurity, and the source and drain were heavily doped with n-type. t_{ox} is the thickness of the oxide layer and L_g represents the gate length. The channel width and body thickness are marked as W and t_b, respectively.

Since the thin p-type body is fully depleted and the mobile

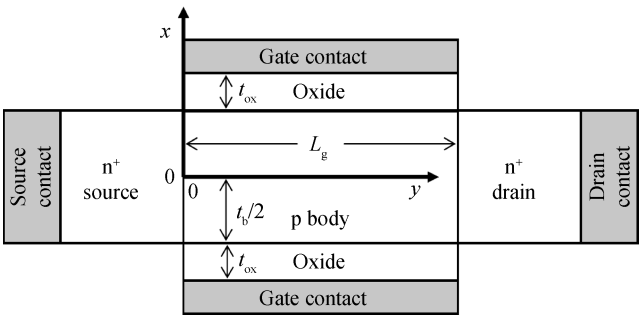

Fig. 1. Schematic view of a DG MOSFET.

* Project supported by the Fund of Liaoning Province Education Department (No. L2012028).
† Corresponding author. Email: xsjin@live.cn
Received 6 April 2012, revised manuscript received 21 June 2012

charge concentration is negligible in the subthreshold region[9], set N_b the body doping concentration, the 2-D Poisson's equation can be written as

$$\frac{\partial^2\psi(x,y)}{\partial x^2}+\frac{\partial^2\psi(x,y)}{\partial y^2}=\frac{qN_b}{\varepsilon_{si}}, \tag{1}$$

where $-t_b/2 \leqslant x \leqslant t_b/2$ and $0 \leqslant y \leqslant L_g$. According to Gauss's Law, on the interface between gate oxide and silicon body, the boundary condition can be written as

$$V_{gs}-V_{fb}-\psi(t_b/2,y)-t_{ox}\frac{\varepsilon_{si}}{\varepsilon_{ox}}\left.\frac{\partial\psi(t_b/2,y)}{\partial x}\right|_{x=t_b/2}=0. \tag{2}$$

And due to symmetry, potential distribution should be an even function, that means

$$\left.\frac{\partial\psi(x)}{\partial x}\right|_{x=0}=0. \tag{3}$$

The boundary condition near the drain / source contact can be written as

$$\psi(x,L_g)=V_{ds}+\phi_{bi}, \tag{4}$$

$$\psi(x,0)=\phi_{bi}, \tag{5}$$

where ϕ_{bi} is the built-in voltage. A simple way to solve this 2-D Poisson's equation is using variable separation technique, based on which the 2-D potential can be divided into 2 functions as

$$\psi(x,y)=\phi_I(x)+\phi_{II}(x,y), \tag{6}$$

where $\phi_I(x)$ is a 1-D function about x, and $\phi_{II}(x,y)$ is a 2-D function about x and y, These two functions should satisfy the following equations and corresponding boundary conditions, respectively.

$$\frac{\partial^2\phi_I(x)}{\partial x^2}=\frac{qN_b}{\varepsilon_{si}}, \tag{7}$$

$$V_{gs}-V_{fb}-\phi_I(t_b/2)-t_{ox}\frac{\varepsilon_{si}}{\varepsilon_{ox}}\frac{\partial\phi_I(t_b/2)}{\partial x}=0, \tag{8}$$

$$\left.\frac{\partial\phi_I(x)}{\partial x}\right|_{x=0}=0, \tag{9}$$

and

$$\frac{\partial^2\phi_{II}(x,y)}{\partial x^2}+\frac{\partial\phi_{II}(x,y)}{\partial y^2}=0, \tag{10}$$

$$-\phi_{II}(t_b/2,y)-t_{ox}\frac{\varepsilon_{si}}{\varepsilon_{ox}}\frac{\partial\phi_{II}(t_b/2,y)}{\partial x}=0, \tag{11}$$

$$\frac{\partial\phi_{II}(t_b/2,y)}{\partial x}=0, \tag{12}$$

$$\phi_{II}(x,L_g)=V_{ds}+\phi_{bi}-\phi_I(x), \tag{13}$$

$$\phi_{II}(x,0)=\phi_{bi}-\phi_I(x). \tag{14}$$

After solving Eq. (7), the 1-D function about x can be analytically expressed as

$$\phi_I(x)=\frac{qN_b}{2\varepsilon_{si}}x^2+V_{gs}-V_{fb}-\frac{qN_b}{2\varepsilon_{si}}\frac{t_b^2}{4}-t_{ox}\frac{qN_bt_b}{2\varepsilon_{ox}}, \tag{15}$$

and the solution of Eq. (10) is a 2-D function about x and y and can be analytically expressed as

$$\phi_{II}(x,y)=\sum_{n=1}^{\infty}\left[A_n\exp\left(\frac{\gamma_n}{t_b/2}y\right)+B_n\exp\left(-\frac{\gamma_n}{t_b/2}y\right)\right]\times\cos\left(\frac{\gamma_n}{t_b/2}x\right), \tag{16}$$

where A_n and B_n are the coefficients coming from the derivation of Eq. (10), they can be expressed as

$$\begin{aligned}A_n=&\frac{1}{2}\sinh^{-1}\left(\frac{\gamma_nL_g}{t_b/2}\right)\times\left[\frac{\sin(2\gamma_n)}{2\gamma_n}+1\right]^{-1}\\&\times\left[1-\exp\left(-\frac{\gamma_nL_g}{t_b/2}\right)\right]\\&\times\left[\left(V_{bi}-V_{gs}+V_{fb}+\frac{qN_bt_{ox}t_b}{2\varepsilon_{ox}}+\frac{qN_bt_b^2}{4\varepsilon_{si}\gamma_n^2}\right)\frac{2}{\gamma_n}\sin\gamma_n\right.\\&\left.-\frac{t_b^2}{4\gamma_n^2}\frac{2qN_b}{\varepsilon_{si}}\cos\gamma_n\right]+\frac{1}{2}\sinh^{-1}\left(\frac{\gamma_nL_g}{t_b/2}\right)\\&\times\left[\frac{\sin(2\gamma_n)}{2\gamma_n}+1\right]^{-1}\times V_{ds}\times\frac{2}{\gamma_n}\times\sin\gamma_n,\end{aligned} \tag{17}$$

and

$$\begin{aligned}B_n=&-\frac{1}{2}\sinh^{-1}\left(\frac{\gamma_nL_g}{t_b/2}\right)\times\left[\frac{\sin(2\gamma_n)}{2\gamma_n}+1\right]^{-1}\\&\times\left[1-\exp\left(\frac{\gamma_nL_g}{t_b/2}\right)\right]\\&\times\left[\left(V_{bi}-V_{gs}+V_{fb}+\frac{qN_bt_{ox}t_b}{2\varepsilon_{ox}}+\frac{qN_bt_b^2}{4\varepsilon_{si}\gamma_n^2}\right)\frac{2}{\gamma_n}\sin\gamma_n\right.\\&\left.-\frac{t_b^2}{4\gamma_n^2}\frac{2qN_b}{\varepsilon_{si}}\cos\gamma_n\right]-\frac{1}{2}\sinh^{-1}\left(\frac{\gamma_nL_g}{t_b/2}\right)\\&\times\left[\frac{\sin(2\gamma_n)}{2\gamma_n}+1\right]^{-1}\times V_{ds}\times\frac{2}{\gamma_n}\times\sin\gamma_n.\end{aligned} \tag{18}$$

We can see that A_n and B_n are decided by material parameters such as ε_{ox} and ε_{si}, and design parameters such as L_g, N_b, t_{ox}, t_b. Also, and the influence of biases such as V_{ds} and V_{gs} can also be reflected from them. There is another key coefficient γ_n which is obtained from the following equation,

$$\tan(\gamma+n\pi)=\frac{\varepsilon_{ox}t_b}{2\varepsilon_{si}t_{ox}\gamma}. \tag{19}$$

It's the periodic nth root of this equation. From Eq. (19) we can see that γ_n is decided by the permittivity and thickness of both silicon and oxide. Besides, it's also a key factor to

determine A_n and B_n. Once A_n, B_n and γ_n are decided, the 2-D function $\phi_{\rm II}(x, y)$ can be decided by substituting them back into Eq. (16), too. It should be declared that Equation (16) is a convergence series function, that means only the upper several items of A_n, B_n and γ_n remain and the result is accurate enough for scientific calculations.

The drain-to-source current can be expressed as

$$I_{\rm d} = W \int_{-t_{\rm b}/2}^{t_{\rm b}/2} {\rm d}x J, \tag{20}$$

where J is the current density that contains both drift and diffusion components. It can be written as

$$J = -q\mu_{\rm n} n(x, y) \frac{{\rm d}\psi_{\rm f}(y)}{{\rm d}y}, \tag{21}$$

where $\psi_{\rm f}$ is the quasi-Fermi potential and it is only a function along the channel direction from 0 around the source side to $V_{\rm ds}$ around the drain side. $n(x, y)$ represents the 2-D electron concentration distribution. $\mu_{\rm n}$ is the effective mobility of the electron which is assumed to be a constant in this paper. The total current along source/drain direction can be calculated by integrating the current density in the body thickness (x) direction. Substituting Eq. (21) into Eq. (20) yields that

$$I_{\rm d} = -W \int_{-t_{\rm b}/2}^{t_{\rm b}/2} q\mu_{\rm n} n(x, y) \frac{{\rm d}\psi_{\rm n}(y)}{{\rm d}y} {\rm d}x. \tag{22}$$

Here, the electron concentration can be expressed as a function of the difference between potential and quasi-Fermi potential at a certain place

$$n(x, y) = n_{\rm i} \exp\{q[\psi(x, y) - \psi_{\rm n}(y)]/kT\}. \tag{23}$$

Due to current continuity in y direction, $I_{\rm d}$ should be independent of y. Substituting Eq. (23) into Eq. (22), the drain-to-source current can be expressed as

$$I_{\rm d} = \frac{kTW\mu_{\rm n} n_{\rm i}[1 - \exp(-qV_{\rm ds}/kT)]}{\displaystyle\int_0^{L_{\rm g}} \frac{{\rm d}y}{\displaystyle\int_{-t_{\rm b}/2}^{t_{\rm b}/2} \exp[q\psi(x, y)/kT]{\rm d}x}}. \tag{24}$$

Substituting the function of potential distribution derived above into Eq. (24), the current of DG MOSFETs can be easily calculated.

3. Model verification

It should be noted that the series in Eq. (16) is convergence, and we found that it's accurate enough to be left with only 4 items for calculations. Figure 2 shows the comparison of constant potential contours between our model and 2-D simulation results. It verifies that our model can exactly reflect the body potential distribution in the subthreshold region. The figure also shows that the minimum value of potential is located near the middle between source and drain.

We have verified the subthreshold $I_{\rm d}$–$V_{\rm gs}$ characteristics with simulation results at a fixed body thickness. From Fig.3 we can see that, for 40 nm channel length, the slope of $I_{\rm d}$–$V_{\rm gs}$ curves in the subthreshold region is not seriously influenced by the shortened channel length, however, when the channel

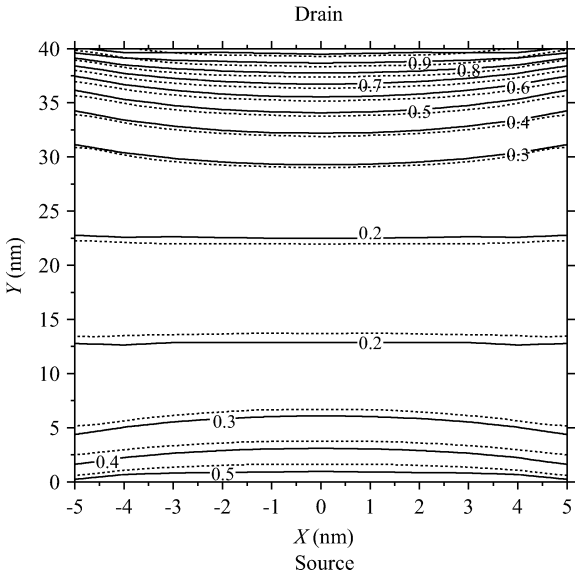

Fig. 2. Comparison of constant potential contours between the proposed model (solid curves) and simulation results (dashed curves) for fin body of DG MOSFETs. $V_{\rm ds} = 0.5$ V, $V_{\rm gs} = 0.2$ V, $a = t_{\rm b}/2 = 5$ nm, $t_{\rm ox} = 1.5$ nm, $L_{\rm g} = 40$ nm, and $N_{\rm b} = 10^{18}$ cm^{-3}.

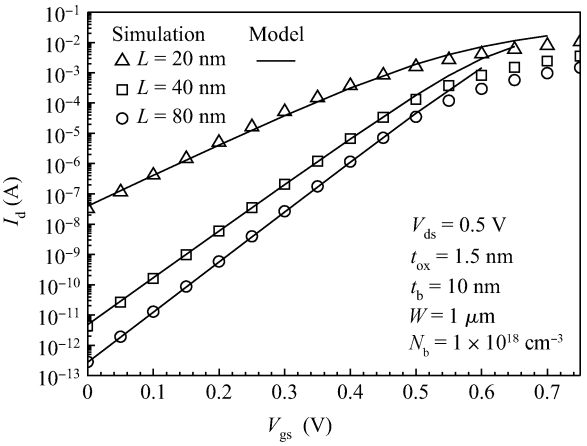

Fig. 3. Comparison of $I_{\rm d}$–$V_{\rm gs}$ curves between the proposed model (curves) and simulation results (symbols) with different channel lengths.

length reduced to 20 nm, the subthreshold slope is seriously decreased. This figure also proves that our model can exactly reflect the characteristics' degradation due to deep nanoscale short channel.

Figure 4 shows the comparison of $I_{\rm d}$–$V_{\rm gs}$ curves between the proposed model and simulation results (lines) with different body thicknesses. We can see that the body thickness affects the properties of $I_{\rm d}$–$V_{\rm gs}$ curves in the subthreshold region. The current increases almost 10 times as the body thickness increases with the same biases conditions, and it's proved that reducing the body thickness to make the silicon body thinner is a good method to improve the subthreshold slope characteristics for deep nanoscale channel length DG MOSFETs. Also, for both undoped and doped cases, our model matches well with the simulation results.

Figure 5 is a comparison of $I_{\rm d}$–$V_{\rm gs}$ curves between the pro-

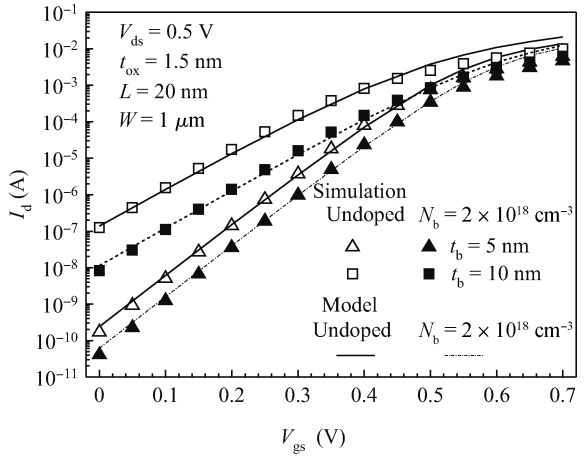

Fig. 4. Comparison of I_d–V_{gs} curves between the proposed model (curves) and simulation results (symbols) with different body thicknesses.

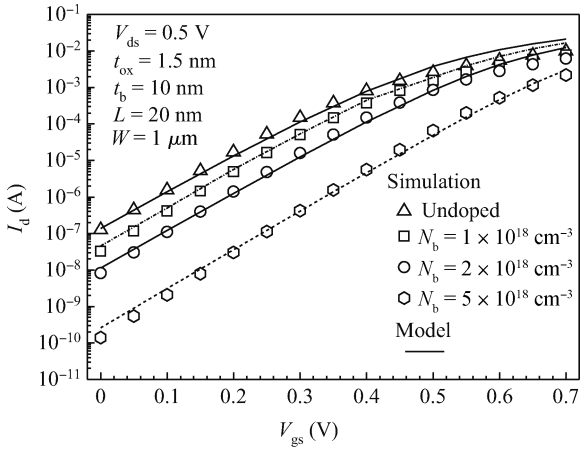

Fig. 5. Comparison of I_d–V_{gs} curves between the proposed model (curves) and simulation results (symbols) with different body doping concentrations.

posed model and simulation results with different body doping concentrations. From this figure, we can see that doping concentration can not obviously affect the subthreshold slope, but the intensity of current which means it can be an effective design parameter to adjust the threshold voltage of DG MOSFETs. This figure also proved that our model is proper for both undoped and doped cases. The model is effective and matches well with simulations' results for the doping concentration N_b shifts from intrinsic to 5×10^{18} cm^{-3}.

4. Conclusion

A model of subthreshold characteristics for both undoped and doped deep nanoscale short channel double-gate (DG) MOSFETs has been developed. The body potential distribution was directly derived by solving the 2-D Poisson's equation using variable separation technique. The proposed models can exactly and directly reflect the degraded subthreshold characteristics due to nanoscale channel length without any fitting parameters. Design parameters such as body thickness, gate oxide thickness, body doping concentrations and so on are also considered, which also can be directly reflected from our proposed model. The models have been verified by comparing with device simulations' results and can be used in circuit simulation and characteristics evaluation of DG MOSFETs.

References

[1] Gao Y, Yang J, Yang Y, et al. Characteristics of vertical double-gate dual-strained-channel MOSFETs. Journal of Semiconductors, 2009, 30: 064002
[2] Yao G, Luo X, Wang Q, et al. Novel SOI double-gate MOSFET with a p-type buried layer. Journal of Semiconductors, 2012, 33: 054006
[3] Taur Y, Liang X, Wang W, et al. A continuous, analytic drain-current model for DG MOSFETs. IEEE Electron Device Lett, 2004, 25: 107
[4] Lu H, Taur Y. An analytic potential model for symmetric and asymmetric DG MOSFETs. IEEE Trans Electron Devices, 2006, 53: 1161
[5] Yu B, Lu H, Liu M, et al. Explicit continuous models for double-gate and surrounding-gate MOSFETs. IEEE Trans Electron Devices, 2007, 54: 2715
[6] Lu H, Yu B, Taur Y. A unified charge model for symmetric double-gate and surrounding-gate MOSFETs. Solid-State Electron, 2008, 52: 67
[7] Liu F, He J, Zhang J, et al. A non-charge-sheet analytic model for symmetric double-gate MOSFETs with smooth transition between partially and fully depleted operation modes. IEEE Trans Electron Devices. 2008, 55: 3494
[8] Jin X, Liu X, Lee J, et al. A continuous current model of fully-depleted symmetric double-gate MOSFETs considering a wide range of body doping concentrations. Semicond Sci Technol, 2010, 25: 055018
[9] Liang X, Taur Y. A 2-D analytical solution for SCEs in DG MOSFETs. IEEE Trans Electron Devices, 2004, 51: 1385
[10] Hamid H, Guitart J, Iñíguez B. Two-dimensional analytical threshold voltage and subthreshold swing models of undoped symmetric double-gate MOSFETs. IEEE Trans Electron Devices, 2007, 54: 1402
[11] Ray B, Mahapatra S. Modeling of channel potential and subthreshold slope of symmetric double-gate transistor. IEEE Trans Electron Devices, 2009, 56: 260
[12] Monga U, Fjeldly T. Compact subthreshold current modeling of short-channel nanoscale double-gate MOSFET. IEEE Trans Electron Devices, 2009, 56: 1533
[13] Cerdeira A, Iñíguez B, Estrada M. Compact model for short channel symmetric doped double-gate MOSFETs. Solid-State Electron, 2008, 52: 1064
[14] SILVACO International. ATLAS User's Manual, 2005